Journal of Sound and Vibration 328 (2009) 243–258

Contents lists available at ScienceDirect

Journal of Sound and Vibration

journal homepage: www.elsevier.com/locate/jsvi

Acoustic radiation from a simple structure in supersonic flow

Peter L. Schmidt [a,*], Kenneth D. Frampton [b]

[a] Department of Engineering Technology, The University of North Carolina at Charlotte, 9201 University City Boulevard, Charlotte, NC 28223-000, USA
[b] Institute of Sound and Vibration Research, University of Southampton, University Road, Highfield, Southampton SO17 1BJ, UK

ARTICLE INFO

Article history:
Received 1 September 2006
Received in revised form
3 August 2009
Accepted 5 August 2009
Handling Editor: C.L. Morfey
Available online 1 September 2009

ABSTRACT

It is well established that fluid flow can have significant effects on structural acoustic behavior, as is the fact that induced coupling between discrete modes of vibration becomes significant as flow velocity increases. To date, work in this area has been confined to subsonic flows, with the effects on sound radiation efficiency and sound power radiation quantified and compared for various subsonic flow speeds. The purpose of this work is to study the effects that supersonic flow has on these structural acoustic phenomena, along with an investigation of the uncoupled behavior of single modes in the transonic region. Theoretical development of the equations governing the vibration of a simply supported plate in an infinite baffle and an aerodynamic system that models a semi infinite flowing medium along with the method for coupling these systems is included. Computational results are presented illustrating the behavior of the uncoupled modes in the transonic region and the uncoupled and coupled effects on the structural response and sound power radiation as well as a study of the radiation efficiency of the coupled system.

1. Introduction

Acoustic radiation from simple vibrating structures, such as plates [1], shells and cylinders [2], into stationary fluids is well understood [3]. However, little has been done to date concerning structural acoustic radiation into a fluid that is moving with a steady, constant motion. Of the few available references that do address radiation into a convected fluid only a very few include flow-induced structural modal coupling. Yet, such flow induced coupling is well understood in the field of aeroelasticity [4] and is known to cause substantial changes in dynamic behavior culminating in static or dynamic instabilities [5]. Such instabilities may not be of specific concern in structural acoustics. However, these flow-induced changes in dynamic response become significant well away from the stability boundaries and may well be important to structural acoustic analysis.

As stated, a few investigations have been published which address sound radiation from convected fluid-loaded plates. Work by Abrahams provided a solution to the convected wave equation using asymptotic techniques [6]. Atalla and Nicolas [7] calculated the radiation impedance for a piston in the presence of flow and noted that the radiation resistance increased and the radiation reactance decreased with increasing flow. Similar conclusions were drawn for a simply supported plate vibrating in the (1, 1) and (2, 2) modes. Graham [8] noted a decrease in the critical frequency of plate modes in the presence of flow. One of the authors published analysis of the effect of convected fluid loading on radiation efficiency [9] and a subsequent work on the effect of flow induced coupling [10]. The basic conclusions from these two works were that as flow

* Corresponding author. Tel.: +1 704 687 2979; fax: +1 704 687 6577.
E-mail addresses: pschmid3@uncc.edu, peter.leo.schmidt@gmail.com (P.L. Schmidt).

0022-460X/$ - see front matter © 2009 Elsevier Ltd. All rights reserved.
doi:10.1016/j.jsv.2009.08.005

speed increases the radiation efficiency increases and the frequency at which the plate becomes an efficient radiator of sound decreases. The cause of the increase in radiation efficiency was found to be an effective increase in plate phase velocity for structural waves traveling upstream relative to the flow. Equivalently, the radiating wavenumber region broadens as flow velocity increases, reaching an infinite width as Mach number approaches unity. While each of the studies mentioned above noted increases in radiated sound as a result of flow, only [10] considered the effects of flow-induced coupling.

A few publications are available that consider the effects of coupling with flow. Sgard et al. [11] used a finite element approach along with the extended Kirchoff integral to calculate the power radiated from a vibrating plate into a convected fluid. They, too, noted an increase in radiated sound power with increasing flow speed. Wu and Maestrello [12] also included flow-induced coupling when calculating the radiated acoustic pressure. However, radiated sound power was not specifically discussed since the focus was on stability analysis. For analysis of the non-convected case, see Frendi et al. [13].

The objective of this work is to quantify the sound power radiated from a rectangular, simply supported plate subject to a supersonic convected fluid on one surface and a vacuum on the other. Consideration of supersonic flow is important since low convection velocities are among the first simplifications used to attempt purely analytical solutions to the problem of acoustic radiation coupled with convection [3] yet tools for analysis are needed to accommodate renewed interest in supersonic passenger aircraft [14]. While others have studied the structural effects generated by the shock waves associated with supersonic flow [15], this work assumes that any shocks are located well away from the structure under analysis and that the interaction with the flow is not affected.

Of particular importance to this effort is the inclusion of flow-induced structural modal coupling. The discussion begins with the dynamic modeling of the plate followed by a summary of the solution to the convected wave equation subject to the boundary conditions of a vibrating plate in an infinite baffle. A method casting the aerodynamic model in state space form is provided, along with an algorithm for creating a reduced order version of the aerodynamic model. Next, the method for calculating the radiated sound power is described. Numerical results are presented which indicate the effect of convected fluid loading on the structural response, radiated sound power and radiation efficiency of the simple structure.

2. Dynamics of the structure

The simple structure considered here is a finite, elastic, rectangular plate, embedded in an infinite baffle, as shown in Fig. 1. On one side of the plate is a semi-infinite fluid, flowing parallel to the mid-plane of the plate in the positive x-axis direction. The other side of the plate is exposed to a vacuum.

The plate is modeled by employing Galerkin's technique to discretize the linear equations of motion [16]. The partial differential equation of motion for a thin, uniform plate is [17]

$$0 = D\nabla^4 w(x,y,t) + \rho h \frac{\partial^2 w(x,t)}{\partial t^2} + p(x,y,t) + p_d(x,y,t), \tag{1}$$

where $w(x,y,t)$, D, ρ and h are the panel displacement, stiffness, density and thickness, respectively. The plate is forced by the pressure fluctuations in the fluid caused by plate motion, $p(x,y,t)$, and an independent disturbance pressure, $p_d(x,y,t)$.

A separable solution is assumed using the in vacuo plate eigenfunctions and generalized coordinates of the form

$$w(x,y,t) = \sum_{n=1}^{N} \psi_n(x,y) q_n(t), \tag{2}$$

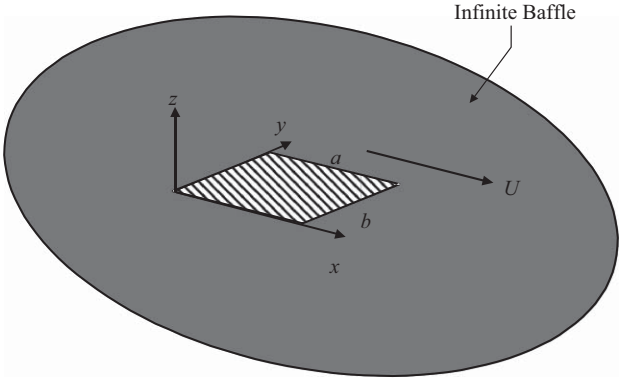

Fig. 1. Schematic of a plate in an infinite baffle.

where $\psi_n(x,y)$ is the mode shape, $q_n(t)$ is the generalized coordinate and N is the number of structural modes considered in the analysis. The velocity of the plate can also be represented using the plate eigenfunctions and generalized coordinates as

$$\dot{w}(x,y,t) = \sum_{n=1}^{N} \psi_n(x,y)\dot{q}_n(t). \tag{3}$$

The approach presented here can accommodate any plate boundary condition. However, results will be presented for a simply supported plate, which has been shown to have the following in vacuo mode shapes [17]:

$$\psi_n(x,y) = \sin\left(\frac{j\pi}{a}x\right)\sin\left(\frac{k\pi}{b}y\right), \tag{4}$$

where the nth plate mode has (x,y) directional indices (j,k).

Substituting Eqs. (2) and (4) into Eq. (1) and multiplying by an arbitrary expansion function, $\psi_m(x,y)$, yields the homogeneous form:

$$D\sum_{n=1}^{N} \nabla^4\psi_n\psi_m q_n + \rho\sum_{n=1}^{N} \psi_n\psi_m\ddot{q}_n = 0. \tag{5}$$

Eq. (5) can be written in integral form for a single mode. The individual homogeneous equations are of the form

$$Dq_n\int_S(\nabla^4\psi_n)\psi_n\,\mathrm{d}S + \rho\ddot{q}_n\int_S\psi_n\psi_n\,\mathrm{d}S = 0. \tag{6}$$

Eq. (6) can be rewritten in the familiar form:

$$M_n\ddot{q}_n + K_n q_n = 0, \tag{7}$$

where

$$M_n = \rho\int_S\psi_n\psi_n\,\mathrm{d}S \tag{8}$$

and

$$K_n = D\int_S(\nabla^4\psi_n)\psi_n\,\mathrm{d}S. \tag{9}$$

Substituting Eq. (4) into (8) and (9) results in

$$M_n = \rho\int_0^a\int_0^b \sin^2\left(\frac{j\pi x}{a}\right)\sin^2\left(\frac{k\pi y}{b}\right)\mathrm{d}x\,\mathrm{d}y \tag{10}$$

and

$$K_n = D\pi^4\left(\frac{j^2}{a^2}+\frac{k^2}{b^2}\right)^2\int_0^a\int_0^b \sin^2\left(\frac{j\pi x}{a}\right)\sin^2\left(\frac{k\pi y}{b}\right)\mathrm{d}x\,\mathrm{d}y. \tag{11}$$

Eqs. (6)–(11) arise from the assumption that the expansion functions are equal to the eigenfunctions of the structure (Eq. (4)), with m and n also representing the x and y modal indices. Integrating over the domain using the stated boundary conditions yields

$$M_n = \frac{ab\rho}{4} \tag{12}$$

and

$$K_n = \frac{D\pi^4 ab}{4}\left(\frac{j^2}{a^2}+\frac{k^2}{b^2}\right)^2, \tag{13}$$

where the nth term applies to the mode with indices (j,k). M_n is referred to as the modal mass term, and K_n is referred to as the modal stiffness term.

With these relationships in hand, a set of ordinary differential equations of the form

$$0 = M_n[\ddot{q}_n(t) + 2\xi\omega_n\dot{q}_n(t) + \omega_n^2 q_n(t)] + Q_n(t) + Q_n^d(t), \tag{14}$$

can be written. A damping term has been added to the non-homogeneous equation to account for energy dissipation in the structure. The generalized force terms, Q_n and Q_n^d are discussed below.

3. State space form of the structural model

Eq. (14) actually represents N simultaneous ordinary differential equations where N is the number of structural modes used in the solution. In order to facilitate integration of Eq. (14) with the fluid dynamics, it is cast in state variable form such that [18]

$$\dot{\mathbf{x}}_\mathbf{s} = \mathbf{A}_\mathbf{s}\mathbf{x}_\mathbf{s} + \mathbf{B}_\mathbf{s}\mathbf{u}_\mathbf{s},$$

$$\mathbf{y}_\mathbf{s} = \mathbf{C}_\mathbf{s}\mathbf{x}_\mathbf{s}. \tag{15}$$

The $\mathbf{A}_\mathbf{s}$ and $\mathbf{B}_\mathbf{s}$ matrices are populated with the coefficients of Eq. (14) while the state, input and output vectors $\mathbf{x}_\mathbf{s}$, $\mathbf{u}_\mathbf{s}$ and $\mathbf{y}_\mathbf{s}$ are defined as

$$\mathbf{x}_\mathbf{s} = \{q_1(t)\cdots q_N(t)\ \ \dot{q}_1(t)\cdots\dot{q}_N(t)\}^{\mathrm{T}}, \tag{16}$$

$$\mathbf{u}_\mathbf{s} = \{Q_1(t)\cdots Q_N(t)\ \ Q_1^d(t)\cdots Q_N^d(t)\}^{\mathrm{T}}, \tag{17}$$

and

$$\mathbf{y}_\mathbf{s} = \mathbf{x}_\mathbf{s} = \{q_1(t)\cdots q_N(t)\ \ \dot{q}_1(t)\cdots\dot{q}_N(t)\}^{\mathrm{T}}. \tag{18}$$

The disturbance generalized forces are given by

$$Q_n^d(t) = \int_0^b\int_0^a p_d(x,y,z=0,t)\psi_n(x,y)\,\mathrm{d}x\,\mathrm{d}y, \tag{19}$$

and the fluid generalized forces are defined by

$$Q_n(t) = \int_0^b\int_0^a p(x,y,z=0,t)\psi_n(x,y)\,\mathrm{d}x\,\mathrm{d}y, \tag{20}$$

where $p_a(x,y,z=0,t)$ is the fluid pressure acting on the plate due to plate motion and $Q_n(t)$ is the resulting generalized force. This generalized force is due entirely to the fluid response created by plate motion and is therefore the mechanism through which modal coupling is created. Developing an expression for this generalized force is the next step toward studying the effects of flow on sound radiation.

4. Aerodynamic model

Other investigators have used two different approaches to find the acoustic pressure that acts on the surface of a vibrating plate. One approach is the Helmholtz–Kirchoff integral, typically solved using numerical methods [7,19,11]. An alternate method involves spatial Fourier transform techniques that require approximate inverse transforms derived using asymptotic techniques [6,8]. The approach detailed here is based on the Fourier transform method.

The generalized forces due to aerodynamic pressure in Eq. (14) are obtained by solving the partial differential equation that describes the velocity potential in an inviscid, irrotational fluid flow in the x direction, as shown in Fig. 1. This relationship is also known as the convected wave equation:

$$\nabla^2\phi - \frac{1}{c^2}\left[\frac{\partial^2\phi}{\partial t^2} + 2U\frac{\partial^2\phi}{\partial t\,\partial x} + U^2\frac{\partial^2\phi}{\partial x^2}\right] = 0. \tag{21}$$

Eq. (21) is subject to the boundary conditions for a plate embedded in an infinite baffle,

$$\left.\frac{\partial\phi}{\partial z}\right|_{z=0} = \begin{cases} U\dfrac{\partial w}{\partial x} + \dfrac{\partial w}{\partial t} & \text{on the plate} \\ 0 & \text{off the plate} \end{cases}, \tag{22}$$

as well as a finiteness condition as z approaches infinity. Here, ϕ, c, and U are the velocity potential, speed of sound and flow velocity, respectively.

The solution to these equations follows the one presented by Dowell [4], and summarized in [9]. The first step is to perform a Laplace transform with respect to time

$$\Phi(x,y,z,s) = \int_0^\infty \mathrm{e}^{-st}\phi(x,y,z,t)\,\mathrm{d}t, \tag{23}$$

and a double Fourier transform with respect to the x and y spatial dimensions, given by

$$\tilde{\Phi}(\alpha,\gamma,z,s) = \int_{-\infty}^{\infty}\int_{-\infty}^{\infty} \mathrm{e}^{-\mathrm{i}(\alpha x+\gamma y)}\Phi(x,y,z,s)\,\mathrm{d}x\,\mathrm{d}y, \tag{24}$$

where s is the Laplace transform variable, $\mathrm{i} = \sqrt{-1}$, and α and γ are the Fourier transform variables in x and y.

If these relationships are applied to Eq. (21), the following is obtained:

$$\frac{\mathrm{d}^2\tilde{\Phi}}{\mathrm{d}z^2} = \tilde{\Phi}\mu^2, \tag{25}$$

where

$$\mu = \sqrt{\frac{s^2}{c^2} + \frac{2Ms\,\mathrm{i}\alpha}{c} - \alpha^2(M^2-1) + \gamma^2}. \tag{26}$$

where $M = U/c$ is the Mach number, and the square root is taken to ensure stability and causality [4].

The triple transform of the boundary condition is obtained in a similar way, given by

$$\left.\frac{\mathrm{d}\tilde{\Phi}}{\mathrm{d}z}\right|_{z=0} = [U\,\mathrm{i}\alpha\tilde{W} + s\tilde{W}] \equiv \tilde{F}, \tag{27}$$

where $\tilde{W}$ is the triple transform of the plate displacement, w.

This transformed version of the convected wave equation (Eq. (21)), when solved with the transformed boundary condition of Eq. (27), yields the transformed velocity potential on the plate surface, which is given by

$$\tilde{\Phi}_{|z=0} = \frac{-\tilde{F}}{\mu}\mathrm{e}^{-\mu z} = \frac{-\tilde{F}}{\mu}. \tag{28}$$

If an inverse Laplace transform is taken of Eq. (28), the result is the time domain velocity potential on the surface of the plate,

$$\tilde{\phi}(\alpha,\gamma,z=0,t) = -c\int_0^t \tilde{f}(\alpha,\gamma,\tau)\,\mathrm{e}^{-\mathrm{i}Mc\alpha(t-\tau)}J_0[(\alpha^2+\gamma^2)^{1/2}c(t-\tau)]\,\mathrm{d}\tau, \tag{29}$$

where $J_k[\bullet]$ is a Bessel function of the first kind and of the order k and τ is a variable of integration.

In order to calculate aerodynamic forces on the plate, the pressure on the surface of the plate is needed. The velocity potential is related to the acoustic pressure through Bernoulli's equation:

$$p = -\rho\left[\frac{\partial\phi}{\partial t} + U\frac{\partial\phi}{\partial x}\right], \tag{30}$$

where ρ is the density of the fluid. If Eqs. (29) and (30) are combined, and one makes use of Leibnitz's rule for the differentiation of integrals, the result is

$$\tilde{p}(\alpha,\gamma,z=0,t) = \rho c\tilde{f}(\alpha,\gamma,t) - \rho c^2(\alpha^2+\gamma^2)^{1/2}\int_0^t \tilde{f}(\alpha,\gamma,\tau)\,\mathrm{e}^{-\mathrm{i}Mc\alpha(t-\tau)}J_1[c(\alpha^2+\gamma^2)^{1/2}(t-\tau)]\,\mathrm{d}\tau. \tag{31}$$

An inverse Fourier transform of Eq. (31) can now be performed. A logarithmic singularity exists for subsonic flows at the leading edge of the plate. This presents a problem if it is necessary to determine the pressure at this specific location. However, for this work, only the generalized force due to the aerodynamic pressure is needed. Since the singularity is integrable, the difficulty is avoided [4].

The next step is to substitute Eq. (31) into Eq. (20). Integration with respect to the x and y coordinates is performed next, followed by an inverse Fourier transform with respect to α and γ. This series of operations results in an expression for the generalized forces on the plate such that

$$Q_n = \sum_{m=1}^{N} Q_{mn}(t), \tag{32}$$

where $Q_{mn}(t)$ is the force on the nth plate mode due to the motion of the mth plate mode and N is again the number of structural modes considered in the analysis. The expression for $Q_{mn}(t)$ is given by

$$Q_{mn}(t) = q_m(t)S_{mn} + \dot{q}_m(t)D_{mn} + \int_0^t q_m(\tau)H_{mn}(t-\tau)\,\mathrm{d}\tau + \int_0^t \dot{q}_m(t)I_{mn}(t-\tau)\,\mathrm{d}\tau, \tag{33}$$

with

$$S_{mn} = \frac{1}{M}\int_0^a\int_0^b \frac{\partial\psi_m}{\partial x}\psi_n\,\mathrm{d}x\,\mathrm{d}y, \tag{34}$$

$$D_{mn} = \frac{1}{MU}\int_0^a\int_0^b \psi_m\psi_n\,\mathrm{d}x\,\mathrm{d}y, \tag{35}$$

$$H_{mn}(t) = \frac{U}{4\pi^2 M^2} \int_{-\infty}^{\infty} \int_{-\infty}^{\infty} G_{mn}(\alpha,\gamma)\, \mathrm{i}\alpha \sqrt{\alpha^2+\gamma^2}\, \mathrm{e}^{-\mathrm{i}\alpha U t} J_1(ct\sqrt{\alpha^2+\gamma^2})\, \mathrm{d}\alpha\, \mathrm{d}\gamma, \tag{36}$$

$$I_{mn}(t) = \frac{1}{4\pi^2 M^2} \int_{-\infty}^{\infty} \int_{-\infty}^{\infty} G_{mn}(\alpha,\gamma) \sqrt{\alpha^2+\gamma^2}\, \mathrm{e}^{-\mathrm{i}\alpha U t} J_1(ct\sqrt{\alpha^2+\gamma^2})\, \mathrm{d}\alpha\, \mathrm{d}\gamma, \tag{37}$$

$$G_{mn}(\alpha,\gamma) = \int_0^a \int_0^b \psi_m\, \mathrm{e}^{-\mathrm{i}(\alpha x+\gamma y)}\, \mathrm{d}x\, \mathrm{d}y \int_0^a \int_0^b \psi_n\, \mathrm{e}^{\mathrm{i}(\alpha x+\gamma y)}\, \mathrm{d}x\, \mathrm{d}y. \tag{38}$$

S_{mn} and D_{mn} are referred to as aerodynamic influence coefficients. These terms relate instantaneous changes in structural generalized coordinates to instantaneous changes in the generalized forces due to aerodynamic pressure. The influence coefficients (Eqs. (34) and (35)) can be obtained analytically for most plate eigenfunctions. The same is true of Eq. (38) [9].

The aerodynamic influence functions, $H_{mn}(t)$ and $I_{mn}(t)$, are defined by integrals with no known closed form solution. Dowell [4] used numeric integration to find the influence functions, and then used numeric time stepping algorithms to simulate the system response. This approach worked well for Dowell's area of interest, stability analysis. This work depends on the ability to perform eigenvalue analysis, similar to that done by Currey and Cunefare [20]. This necessitates the use of a singular value decomposition technique, which results in a state variable representation of the fluid dynamic model. This approach allows one to represent the relationship between the motion of the structure and the generalized forces in transfer function form.

5. Approximation of the aerodynamic forces

In order to approximate the aerodynamic generalized forces, a singular value decomposition (SVD) technique originally developed as a system identification tool is applied [21]. This SVD method uses time domain impulse responses to obtain the system representation. Since the aerodynamic influence functions, $H_{mn}(t)$ and $I_{mn}(t)$, are essentially impulse responses of the aerodynamic model, the SVD method is easily applied to the problem at hand. This SVD method also has the advantage of producing a model in state variable form, which is the desired formulation here. This approach also allows the use of standard system analysis tools available based on linear systems theory.

Since a state space model of the aerodynamic subsystem is desired, Eq. (33) must be rewritten in the proper form. Eq. (33) is a mapping of the relationship between the motion of the structure and the aerodynamic forces. This relationship can be expressed in the following form:

$$\mathbf{x}((k+1)T) = \mathbf{A}\mathbf{x}(kT) + \mathbf{B}\mathbf{u}(kT),$$

$$\mathbf{y}(kT) = \mathbf{C}\mathbf{x}(kT) + \mathbf{D}\mathbf{u}(kT), \tag{39}$$

where T is the discrete time increment and k is the time index. The state variable system ($\mathbf{A}$,$\mathbf{B}$,$\mathbf{C}$,$\mathbf{D}$) has n states in $\mathbf{x}$, p inputs in $\mathbf{u}$ and m outputs in $\mathbf{y}$. For the structure considered here with N modes included in the model expansion, the input ($\mathbf{u}$) and output ($\mathbf{y}$) vectors take the form

$$\mathbf{u} = [q_1 \;\; q_2 \;\; \cdots \;\; q_N \;\; \dot{q}_1 \;\; \dot{q}_2 \;\; \cdots \;\; \dot{q}_N]^{\mathrm{T}} \tag{40}$$

and

$$\mathbf{y} = [Q_1 \;\; Q_2 \;\; \cdots \;\; Q_N]^{\mathrm{T}}. \tag{41}$$

The development of this state variable model follows the system identification procedure of Kung [21]. For this work, $m = N$ and $p = 2N$. It begins with the construction of a block Hankel matrix of the system impulse responses. The basic form of this matrix is

$$\mathbf{H} = \begin{bmatrix} \mathbf{h}(T) & \mathbf{h}(2T) & \mathbf{h}(3T) & \cdots & \mathbf{h}((J+1)T) \\ \mathbf{h}(2T) & \mathbf{h}(3T) & \mathbf{h}(4T) & \cdots & 0 \\ \mathbf{h}(3T) & \mathbf{h}(4T) & \mathbf{h}(5T) & \cdots & 0 \\ \vdots & \vdots & \vdots & \ddots & \vdots \\ \mathbf{h}((J+1)T) & 0 & 0 & \cdots & 0 \end{bmatrix}, \tag{42}$$

where the individual elements of the matrix are given by

$$\mathbf{h}(kT)=\begin{cases}\begin{bmatrix} S_{11} & S_{21} & \cdots & S_{N1} & D_{11} & D_{21} & \cdots & D_{N1}\\ S_{12} & S_{22} & \cdots & S_{N2} & D_{11} & D_{22} & \cdots & D_{N2}\\ \vdots & \vdots & \ddots & \vdots & \vdots & \vdots & \ddots & \vdots\\ S_{1N} & S_{2N} & \cdots & S_{NN} & D_{1N} & D_{2N} & \cdots & D_{NN}\end{bmatrix} & \text{for } k=0\\ \begin{bmatrix} H_{11}(kT) & \cdots & H_{N1}(kT) & I_{11}(kT) & \cdots & I_{N1}(kT)\\ H_{12}(kT) & \cdots & H_{N2}(kT) & I_{12}(kT) & \cdots & I_{N2}(kT)\\ \vdots & \ddots & \vdots & \vdots & \ddots & \vdots\\ H_{1N}(kT) & \cdots & H_{NN}(kT) & I_{1N}(kT) & \cdots & I_{NN}(kT)\end{bmatrix} & \text{for } k=1,2,\ldots,J+1\\ \begin{bmatrix}0 & \cdots & 0\\ \vdots & \ddots & \vdots\\ 0 & \cdots & 0\end{bmatrix} & \text{for } k>J+1\end{cases} \tag{43}$$

This results in a Hankel matrix, $\mathbf{H}$, with dimensions $m(J+1)$ by $p(J+1)$.

The next step is to perform the SVD operation on the matrix $\mathbf{H}$. This operation yields

$$\mathbf{H}=U\Sigma V^{\mathrm{T}}=\mathbf{U}\mathbf{V}^{\mathrm{T}}, \tag{44}$$

where $\mathbf{U}$ is an orthogonal matrix containing the eigenvectors of $\mathbf{H}\mathbf{H}^{\mathrm{T}}$, of dimension $m(J+1)$ by $(J+1)$, $\mathbf{V}$ is an orthogonal matrix containing the eigenvectors of $\mathbf{H}^{\mathrm{T}}\mathbf{H}$, of dimension $p(J+1)$ by $(J+1)$, and the singular value matrix is given by

$$\Sigma=\begin{bmatrix}\sigma_1 & & & & & & & \\ & \sigma_2 & & & & & 0 & \\ & & \ddots & & & & & \\ & & & \sigma_r & & & & \\ & & & & \varepsilon_{r+1} & & & \\ & & & & & \varepsilon_{r+2} & & \\ & 0 & & & & & \ddots & \\ & & & & & & & \varepsilon_{J+1}\end{bmatrix}, \tag{45}$$

such that the singular values are arranged in descending order,

$$\sigma_1\geq\sigma_2\geq\cdots\sigma_r\geq\varepsilon_{r+1}\geq\varepsilon_{r+2}\geq\cdots\varepsilon_{J+1}, \tag{46}$$

with

$$\mathbf{U}=U\Sigma^{1/2}\quad\text{and}\quad\mathbf{V}=\Sigma^{1/2}V^{\mathrm{T}}. \tag{47}$$

If the matrix $\mathbf{H}$ has a rank of r, then the singular values $\varepsilon_{r+1},\varepsilon_{r+2},\ldots,\varepsilon_{J+1}$ are equal to zero. If these singular values are non-zero, but very small, $\mathbf{H}$ has a rank very near to r. In this case, the small singular values represent degrees of freedom with negligible contribution to the system response or slight computational noise in the system impulse response. This property of the system realization is used in selecting the order of the final model.

A reduced order system, $(\hat{\mathbf{A}},\hat{\mathbf{B}},\hat{\mathbf{C}},\hat{\mathbf{D}})$, which discards excess degrees of freedom is created. This new system model, of order r, can be obtained by partitioning the output of the SVD operation as

$$\hat{\mathbf{H}}=\begin{bmatrix}\mathbf{U}_{1,1} & \mathbf{U}_{1,2}\\ \mathbf{U}_{2,1} & \mathbf{U}_{2,2}\\ \vdots & \vdots\\ \mathbf{U}_{J,1} & \mathbf{U}_{J,2}\\ \mathbf{U}_{J+1,1} & \mathbf{U}_{J+1,2}\end{bmatrix}\begin{bmatrix}\mathbf{V}_{1,1}^{\mathrm{T}} & \mathbf{V}_{2,1}^{\mathrm{T}} & \cdots & \mathbf{V}_{J,1}^{\mathrm{T}} & \mathbf{V}_{J+1,1}^{\mathrm{T}}\\ \mathbf{V}_{1,2}^{\mathrm{T}} & \mathbf{V}_{2,2}^{\mathrm{T}} & \cdots & \mathbf{V}_{J,2}^{\mathrm{T}} & \mathbf{V}_{J+1,2}^{\mathrm{T}}\end{bmatrix}, \tag{48}$$

where the block matrices $\mathbf{U}$ and $\mathbf{V}$ are sized as follows:

$$\mathbf{U}_{i,1}\text{ are }m\text{ by }r,$$

$$\mathbf{U}_{i,2}\text{ are }m\text{ by }J-r+1,$$

$$\mathbf{V}_{i,1}\text{ are }p\text{ by }r,$$

$$\mathbf{V}_{i,2} \text{ are } p \text{ by } J - r + 1,$$

$$i = 1 : J + 1. \tag{49}$$

Based on these relationships, the reduced order system model is defined as

$$\hat{\mathbf{A}} = \left(\begin{bmatrix} \mathbf{U}_{1,1} \\ \mathbf{U}_{2,1} \\ \vdots \\ \mathbf{U}_{J,1} \end{bmatrix}^T \begin{bmatrix} \mathbf{U}_{1,1} \\ \mathbf{U}_{2,1} \\ \vdots \\ \mathbf{U}_{J,1} \end{bmatrix} \right)^{-1} \begin{bmatrix} \mathbf{U}_{1,1} \\ \mathbf{U}_{2,1} \\ \vdots \\ \mathbf{U}_{J,1} \end{bmatrix}^T \begin{bmatrix} \mathbf{U}_{2,1} \\ \mathbf{U}_{3,1} \\ \vdots \\ \mathbf{U}_{J+1,1} \end{bmatrix}, \tag{50}$$

$$\hat{\mathbf{B}} = \mathbf{V}_{1,1}^{\mathrm{T}}, \tag{51}$$

$$\hat{\mathbf{C}} = \mathbf{U}_{1,1}, \tag{52}$$

and

$$\hat{\mathbf{D}} = \mathbf{h}(0). \tag{53}$$

This reduced order aerodynamic model will receive inputs from the structural subsystem and provide output both to the structure and for use in analysis. It should be noted that the formulation of the reduced order model renders the states of the model as mathematical constructs with no simple physical meaning.

6. Radiated sound power

The plate and fluid systems in state variable form can be assembled into a coupled fluid/structure system as shown in Fig. 2. Note that fluid/structure coupling is created by the dependence of the fluid generalized forces on the plate motion. So, motion in the plate creates a response in the fluid, which in turn creates a force back on the plate. The effect of such coupling is well understood in the field of aeroelasticity [4] which focuses on coupling induced instabilities. These instabilities are not usually of interest in structural acoustics since structures being investigated are designed to avoid them. However, the effects on plate dynamics can occur when the structure is far from instability, therefore affecting structural acoustic behavior.

Contrast this with the uncoupled fluid structure system shown in Fig. 3. The disturbance excites the structure, which then provides input to the aerodynamic model without feedback to the structural system. This prevents the aerodynamic model from affecting the kinetic energy of the structure, simplifying the calculations shown in the following sections for the uncoupled case.

In order to quantify the effects of coupling on acoustic radiation, it is important to clarify the language used to describe the structural response. The term "in vacuo mode" will be used to describe the plate eigenfunctions of Eq. (2). (The in vacuo modes could be more accurately called comparison functions [16] since, in the fully coupled system, they are really just mathematically convenient functions with which to solve the differential equation). The modes of the fully coupled system shown in Fig. 2 will be referred to as *coupled modes*. These are the structural mode shapes that result from solving the eigenvalue problem of the coupled fluid/structure system. Each coupled mode includes degrees of freedom associated with the plate and with the fluid.

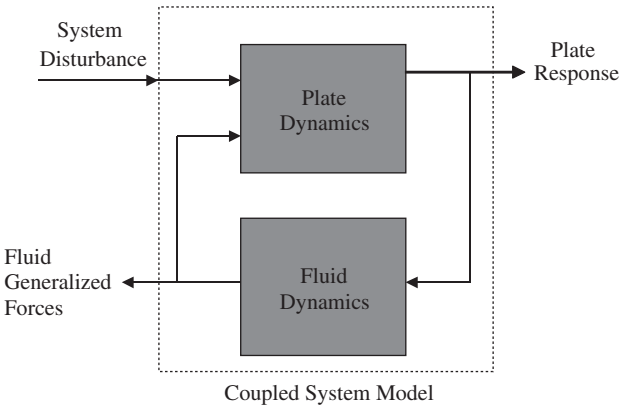

Fig. 2. Schematic of the coupled fluid/structure system.

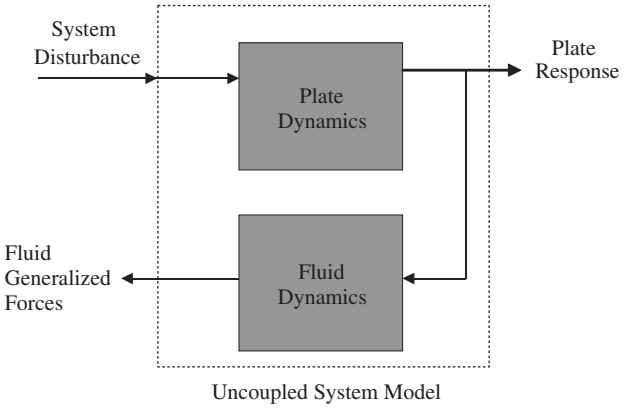

Fig. 3. Schematic of the uncoupled fluid/structure system.

When the fully coupled system is cast in the form shown in Fig. 2, the input/output relationships for the system can be easily manipulated and transfer functions between inputs and system variables can be obtained. This feature of state variable modeling is important for the calculation of radiated sound power.

The instantaneous sound power radiated from the plate can be expressed as [1]

$$\Pi(t) = \int p(x,y,z=0,t)\dot{w}(x,y,t)\,\mathrm{d}S, \tag{54}$$

where $\dot{w}(x,y,t)$ is the velocity of the vibrating plate. By substituting Eq. (2) into Eq. (54) and then making use of Eq. (20), the radiated power can then be expressed as

$$\Pi(t) = \int_S p(x,y,z=0,t)\sum_{n=1}^{N}\psi_n(x,y)\dot{q}_n(t)\,\mathrm{d}S = \sum_{n=1}^{N}\dot{q}_n(t)Q_n(t). \tag{55}$$

Now, the time-averaged radiated power can be expressed as [22]

$$\langle\Pi\rangle = \frac{1}{T}\int_0^T \sum_{n=1}^{N}\dot{q}_n(t)Q_n(t)\,\mathrm{d}t, \tag{56}$$

where T is the period. If harmonic motion is now assumed this expression becomes

$$\langle\Pi\rangle = \sum_{n=1}^{N}\frac{\omega}{2\pi}\int_0^{2\pi/\omega}\mathrm{Re}\{\tilde{Q}_n e^{j\omega t}\}\mathrm{Re}\{\dot{\tilde{q}}_n e^{j\omega t}\}\,\mathrm{d}t = \frac{1}{2}\sum_{n=1}^{N}\mathrm{Re}\{\tilde{Q}_n\dot{\tilde{q}}_n^*\}, \tag{57}$$

where $\dot{\tilde{q}}_n$ and $\tilde{Q}_n$ are the complex magnitudes of the nth modal velocity and nth fluid generalized force, respectively; the asterisk superscript indicates the complex conjugate; $Re\{\,\}$ indicates the real component of the argument; and ω is the excitation frequency. Now making use of system transfer function relationships, the time-averaged radiated sound power can be expressed as

$$\langle\Pi\rangle = \frac{1}{2}\sum_{n=1}^{N}\mathrm{Re}\{I_n(\omega)H_n(\omega)\}|\mathrm{d}(\omega)|^2, \tag{58}$$

where $I_n(\omega)$ is the system transfer function between the disturbance input, $\mathrm{d}(\omega)$, and the fluid generalized force acting on the nth plate mode. The transfer function $H_n(\omega)$ is the system transfer function between the disturbance input and the nth modal velocity. Given the coupled system of Fig. 2, these transfer functions can be readily obtained. Each structural mode is excited by an uncorrelated random signal with a uniform amplitude distribution. This implies that it is uncorrelated in time and in space. This not a particularly realistic excitation, but it is commonly used in structural and control systems analysis and produces a worst case excitation for theoretical study. Note that the use of these transfer function relationships limits the analysis to linear systems. See Peake [23] for analysis of the nonlinear case, but with emphasis on structural stability rather than on acoustical effects.

So the radiated sound power can be calculated by finding the transfer functions of the coupled system, specifying the disturbance spectrum, and carrying out the calculation of Eq. (58). Note that this coupled system can accommodate any disturbance input spectrum desired for analysis. This work uses a white noise input to each individual coupled mode as a disturbance spectrum for the results presented. For alternate approaches, see Maestrello and Linden [24], Frendi and Maestrello [25] and Bauer et al. [26].

7. Transonic radiation efficiency

It must be noted that the use of linearized potential flow (Eq. (21)) is known to be inaccurate in the transonic region. Nonlinearities in the fluid dynamics become significant and should be accounted for. However, there are some interesting and instructive conclusions to be drawn from this linear model. The establishment of more accurate, nonlinear results is left for future work.

The radiation efficiency for a single structural mode, can be expressed as follows [9,19]:

$$\sigma_n = \frac{\langle \Pi_n \rangle}{\rho_0 c_0 ab \langle |\dot{\tilde{q}}_n|^2 \rangle} = 4 \frac{\mathrm{Re}\{\tilde{Q}_n \dot{\tilde{q}}_n^*\}}{\rho_0 c_0 ab}, \tag{59}$$

where Π_n is the radiated power associated with single mode of vibration (Eq. (58)). Use of the transfer function relationship shown in Eq. (59) allows us to obtain the efficiency as a function of frequency. Fig. 4 shows the behavior of the radiation efficiency of the (1, 1) mode at transonic speeds and at two subsonic speeds. Note that the radiation efficiency for $M = 0$ compares well with that found by Wallace [19] and the $M = 0.7$ case compares well with that noted in [8]. In general, the radiation efficiency approaches a magnitude of unity for all frequencies as the speed of sound in the medium is exceeded. Fig. 5 shows the behavior for the (2, 1) mode. Again, the low frequency radiation efficiency increases significantly when the Mach number approaches unity.

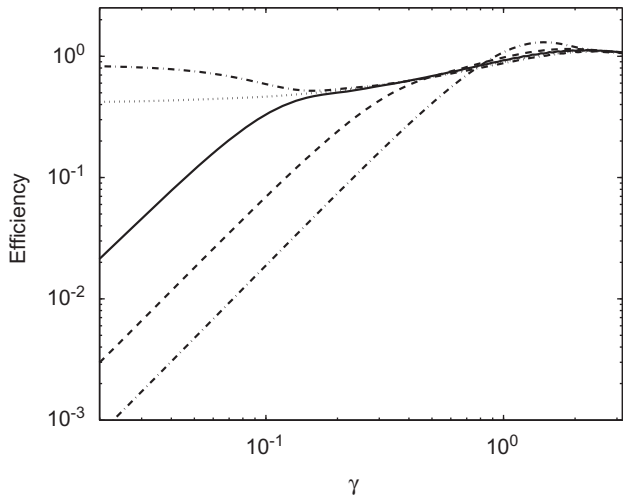

Fig. 4. Radiation efficiency of the (1, 1) mode at selected flow velocities: -·-·-·- $M = 0$, ———— $M = 0.7$, —— $M = 0.9$, · · · · · · · · · $M = 1.0$, and -·-·-·- $M = 1.1$.

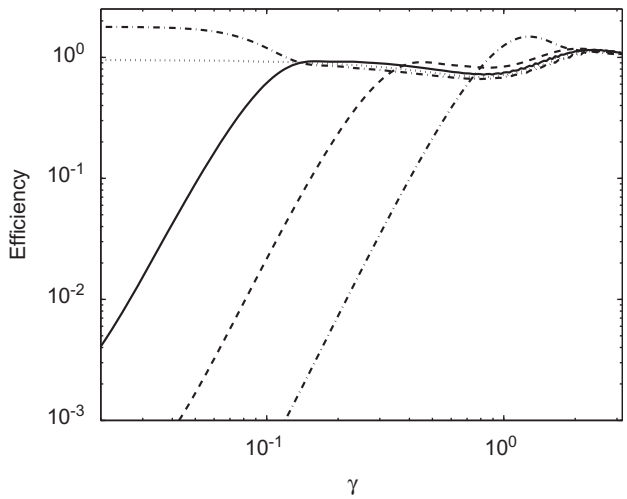

Fig. 5. Radiation efficiency of the (2, 1) mode at selected flow velocities: -·-·-·- $M = 0$, ———— $M = 0.7$, —— $M = 0.9$, · · · · · · · · · $M = 1.0$, and -·-·-·- $M = 1.1$.

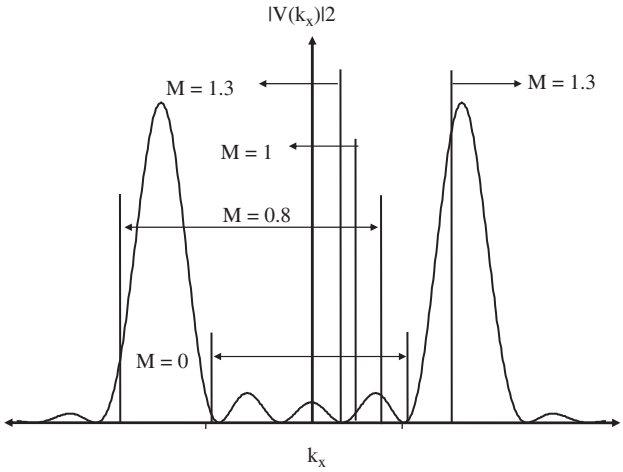

Fig. 6. Wavenumber spectrum of 1-D plate velocity showing the radiating regions for selected Mach numbers.

Increases in radiation efficiency of in vacuo modes without coupling were dealt with previously in [9]. The cause of this increase in radiation efficiency was found to be an effective increase in plate phase velocity for plate waves traveling upstream relative to the flow. Furthermore, the radiating wavenumber region broadens as flow velocity increases, reaching an infinite width as Mach number approaches unity. In the simplified case of a one-dimensional plate the radiating wavenumber region is defined as the region in which the z-components of the wavenumbers are real and positive [9]. This corresponds to

$$\left(\frac{k_z}{k}\right)^2 = 1 - 2M\left(\frac{k_x}{k}\right) + (M^2 - 1)\left(\frac{k_x}{k}\right)^2 > 0. \tag{60}$$

Here k_z is the wavenumber component in the convected fluid normal to the plate, k_x is the wavenumber in the plate, and k is the wavenumber in the fluid. As demonstrated in Eq. (60), the supersonic wavenumber region shifts and expands as Mach number approaches unity from below and becomes (semi-) infinitely wide when $M = 1$. The overall effect in subsonic flow is that, for a fixed wavenumber spectrum in the plate response, as the flow velocity increases more of the plate wavenumber spectrum is enveloped by the radiating region, thus resulting in increased radiation.

When flow becomes supersonic, the radiating regions are strictly positive. Fig. 6 demonstrates this phenomenon for a semi-infinite plate, bounded in x and unbounded in the y direction.

In order for radiation to take place (in supersonic flow),

$$k_x > \frac{k}{M-1} \quad \text{or} \quad k_x < \frac{k}{M+1}. \tag{61}$$

Fig. 6 shows a plot of this equation for the case where $M = 0$ (no flow), 0.8, 1.0 and 1.3. The labeled vertical bars indicate radiating wavenumber regions. Note that the radiating regions are shifted due to the effect of the flow speed on the relationship between the wavenumber in the plate and the wavenumber in the fluid. Also note that for $M = 1.3$ all waves traveling against the flow radiate to the far field. In addition some slower wavenumbers that travel in the direction of the flow radiate as well. While these wavenumbers are not supersonic alone, the speed of the flow makes them supersonic relative to the motion of the fluid. The faster wavenumbers also radiate as one would expect.

8. Computational results

A computational investigation was undertaken based on the theory presented in Sections 1–7. The results presented focus on three areas: the effects of flow-induced coupling on the structural response, the radiated sound power and the behavior of the uncoupled modal radiation efficiency at transonic flow speeds. The physical parameters used were for a plate manufactured from 6061-T6 (UNS A96061) aluminum (density of 2700 kg m^{-3}, thickness of 4 mm, length of 1 m in the direction of flow, width of 0.83 m and modulus of elasticity of 69 GPa) exposed to air at an altitude of 10 km (density of 0.422 kg m^{-3}, speed of sound of 299.5 m s^{-1}). A constant modal damping ratio of 2% was assumed in the formulation of the plate model.

The accuracy of the modeling approach used in this work was established in [10], where results for the subsonic case were presented. In order to ensure accurate results, the plate model of Eq. (14) included 20 modes while the fluid dynamic system of Eq. (32) included 600 degrees of freedom. With this configuration, the plate response and radiated sound power demonstrated sufficient convergence over the first 15 plate modes.

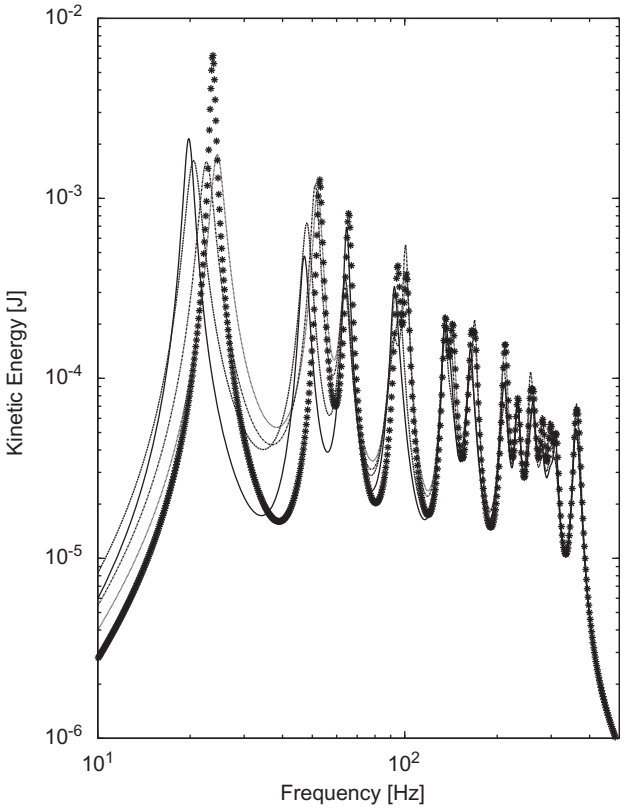

Fig. 7. Structural kinetic energy in supersonic flow: ∗ ∗ ∗ ∗ uncoupled model, —— $M = 0.8$, - - - - - - $M = 1.2$, -·-·-·- $M = 1.5$, and · · · · · · · · · $M = 2.0$.

8.1. *Effect of supersonic flow on structural response*

It is well established that fluid flow can have significant effects on structural acoustic behavior, along with the fact that induced coupling between discrete modes of vibration becomes significant as flow velocity increases. It has also been established that this coupling mechanism is the mechanism for energy flow between distinct modes of vibration in a structure, explaining energy flow into the flowing fluid. Work in this area has been confined to subsonic flows, with the effect on sound radiation efficiency and sound power radiation quantified and compared for various subsonic flow speeds.

The effect of flow on the coupled structural response is demonstrated in Fig. 7, which shows the frequency dependent kinetic energy of the plate for one subsonic and various supersonic flow velocities, as well as the fixed kinetic energy curve associated with the uncoupled model. A general upward shift in fundamental mode frequency is observed as the Mach number increases. This is the opposite of the effect noted for subsonic flow which noted a frequency shift inversely proportional to the flow speed changes [10]. The resonant frequencies of the coupled modes do not change considerably as the Mach number increases above a value of 1.2. The fundamental coupled mode has a resonant frequency of about 18 Hz when $M = 1.2$ moving to 25 Hz when $M = 2.0$. Other modes show small changes in frequency and response amplitude as well. However, other than the fundamental mode frequency shift, the plate energy changes very little with increasing supersonic Mach number. Also note the shift in the fundamental frequency of the structure in the various coupled models versus the one shown and used in the uncoupled case.

8.2. *Effect of supersonic flow on radiated sound power*

The effect of aerodynamic flow on the radiated power from the coupled system is shown in Fig. 8, which shows the radiated sound power as a function of frequency for one subsonic Fig. 8(a) and several supersonic Mach numbers Fig. 8(b)–(d). Note that, while the kinetic energy changed little over the range of supersonic flows, the radiated power curves do change significantly. Overall, the radiated power decreases with increasing flow speed. As convection velocity increases, significant portions of the power flow curve become negative. This behavior indicates energy absorption by the structure rather than radiation. This is a very interesting aspect of the redistribution of energy through flow-induced modal coupling and one that was not noted in subsonic flow. The path through which energy moves from one coupled structural mode to another is the fluid. In this manner the motion of one mode drives other modes, causing them to be out of phase

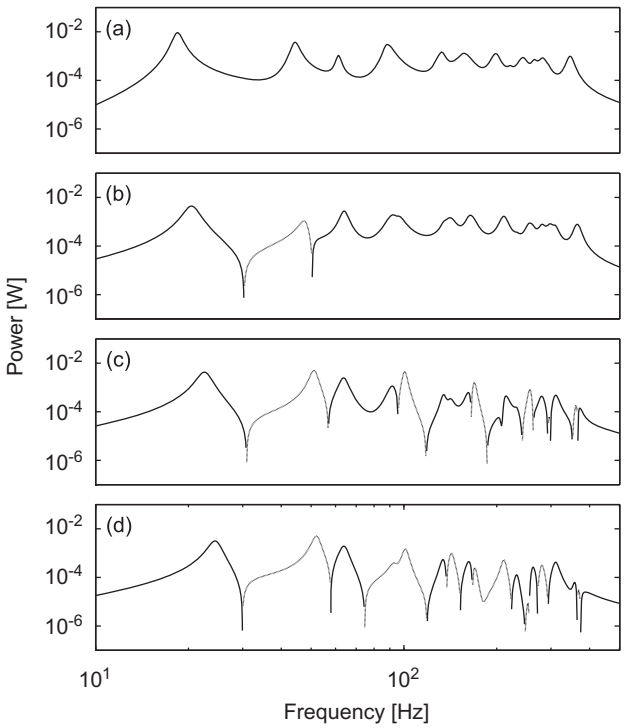

Fig. 8. Radiated sound power in supersonic flow in a coupled model: (a) $M = 0.8$, (b) $M = 1.2$, (c) $M = 1.5$, (d) $M = 2.0$. · · · · · · · · Negative power, and —— positive power.

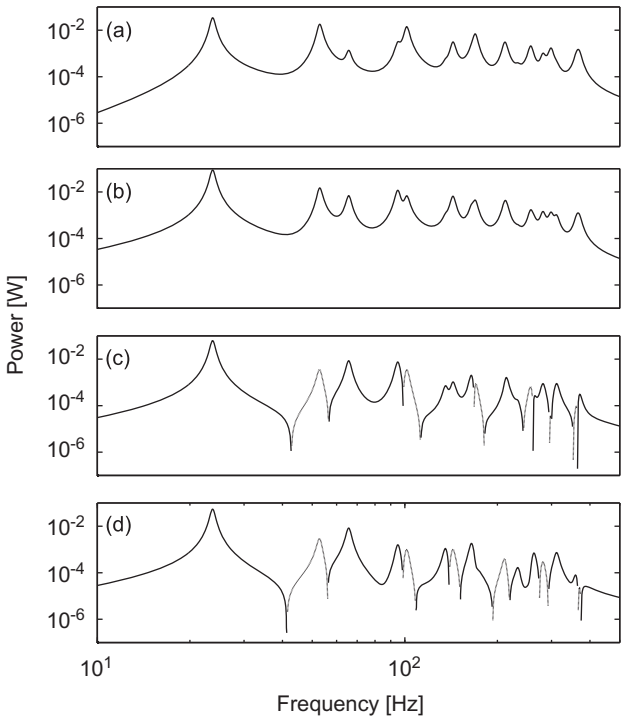

Fig. 9. Radiated sound power in supersonic flow in an uncoupled model: (a) $M = 0.8$, (b) $M = 1.2$, (c) $M = 1.5$, (d) $M = 2.0$. · · · · · · · · Negative power, —— positive power.

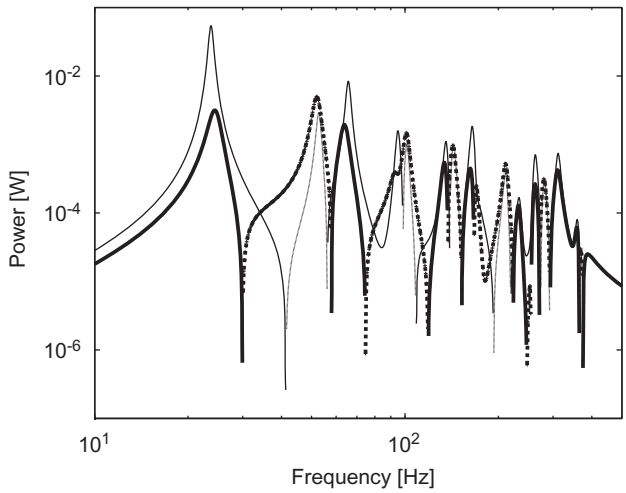

Fig. 10. Comparison of uncoupled and coupled power flow at $M = 2.0$: · · · · · · · · · negative uncoupled power, —— positive uncoupled power, ▬ ▬ negative coupled power, and ▬▬ positive coupled power.

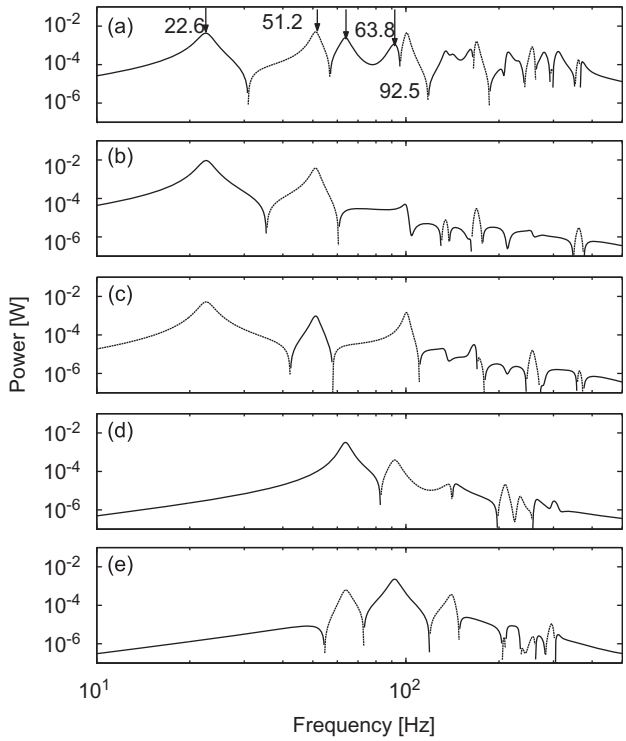

Fig. 11. Modal contributions to radiated sound power when $M = 1.5$: (a) total, (b) first coupled mode, (c) second coupled mode, (d) third coupled mode, (e) fourth coupled mode. · · · · · · · · Negative power, —— positive power.

with the aerodynamic pressure, resulting in negative power flow at some frequencies. This energy is then dissipated by damping in the plate. Fig. 9 repeats the plots shown in Fig. 8, using the uncoupled system model illustrated in Fig. 3. Note that the onset of power absorption by some modes is delayed in the uncoupled model and that the area under the negative portions of the curves is noticeably less than that shown in Fig. 8. The stark differences between coupled an uncoupled behavior are shown in Fig. 10, where the curve for radiated power for the coupled and uncoupled models at a flow velocity of Mach 2 are shown on the same axis. In addition to the reduced power absorption previously mentioned, the uncoupled model also exhibits sharper resonance peaks, especially of the fundamental mode. The coupled model exhibits a highly damped response one would expect from interaction with aerodynamic forces. Fig. 11 also illustrates this behavior by

plotting the total power flow at a selected velocity Fig. 11(a) with the contributions of the first four coupled modes also plotted individually Fig. 11(b)–(e). Subplot Fig. 11(a) also lists the peak frequencies on the kinetic energy plot (Fig. 7) attributable to the associated uncoupled modes for reference.

Clearly, the exchange of energy among modes that occurs in the presence of modal coupling alters not only the dynamic response of the plate but the radiated sound as well. The extent to which coupling affects radiation is demonstrated by the curve for $M = 2.0$ in Fig. 8. Many higher order modes absorb power, causing the total power radiated to the far field to decrease as flow speed rises. Radiated power decreases, and actually becomes negative (i.e., net power is absorbed) as the flow speed approaches Mach 2. The fact that net power flow becomes negative is very interesting in its self. It is not particularly surprising, however, when viewed from an aeroelastic perspective. The fact that fluid/structure coupling can result in dynamic instability is frequently viewed as negative damping in the structure.

8.3. *Effect of supersonic flow on radiation efficiency*

The effect of modal coupling is also illustrated in Fig. 12, which plots the total radiation efficiency versus flow velocity for both the coupled and uncoupled model. Radiation efficiency for a single mode of vibration as a function of frequency is described by Eq. (59). The data shown in Fig. 9 are given by

$$\sigma_T = \sum_{n=1}^{N} \int_0^{\omega_{\max}} \sigma_n \, \mathrm{d}\omega. \tag{62}$$

This quantity is considered as the total radiation efficiency, and is indicative of the ability of the structure to radiate available energy to the far field as a function of frequency.

The total radiation efficiency obtained for the range of flow speeds studied expands on those found in previous work [10]. Rather than increasing with flow speed as previously postulated, the radiation efficiency rises with subsonic flow velocity. Total radiation efficiency peaks at $M = 1.0$ as predicted, and decays with further increase in flow speed. The uncoupled model clearly over-predicts the amount of energy dispersed from the structure to the surrounding flow, due to the assumption of a plate kinetic energy that does not change in amplitude or frequency content with changes in flow velocity. The radiation efficiency, in fact, becomes negative as supersonic convection velocity increases for the coupled case. This behavior illustrates the role of coupling on power flow at high convection velocities and provides further insight into

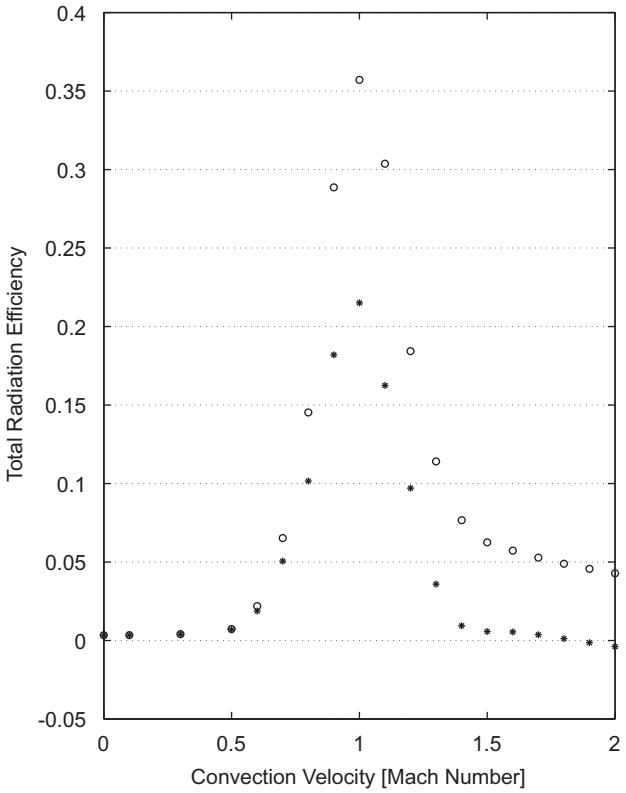

Fig. 12. Total radiation efficiency in supersonic flow for the uncoupled and coupled model: ∗—coupled model and o—uncoupled model.

the effects of convection on structural power flow. Further work is needed to establish the existence of any meaningful connection between the negative power flow noted here and the onset of structural instability.

9. Conclusions

The effect of flow-induced coupling on the radiated sound power from plates has been presented. The modeling of the structure and fluid has been summarized and the effects of flow-induced coupling on the plate response have been described and compared with the uncoupled case. The most notable effect is that the radiated sound power decreases as flow velocities increase from the transonic region. However, the kinetic energy in the plate increases only slightly with flow speed. This behavior is attributable to the flow induced coupling driving some modes out of phase with the aerodynamic model, resulting in decreased radiation. The structure was also shown to be a net absorber of power at very high convection velocities, and that the coupled model demonstrated behavior of the radiation efficiency as predicted by analytical studies done by others.

Acknowledgment

The authors wish to acknowledge the support of the National Science Foundation of the United States through their CAREER grant number 0134224.

References

[1] F. Fahy, *Sound and Structural Vibration*, Academic Press, New York, 1985.
[2] M. Junger, D. Feit, *Structures and their Interaction*, second ed., MIT Press, Cambridge, MA, 1986.
[3] M. Howe, *Acoustics of Fluid Structure Interactions*, Cambridge University Press, Cambridge, UK, 1998.
[4] E. Dowell, *Aeroelasticity of Plates and Shells*, Noordhoff International Publishing, The Netherlands, 1975.
[5] N. Peake, On the unsteady motion of a long fluid loaded elastic plate with mean flow, *Journal of Fluid Mechanics* 507 (2004) 335–366.
[6] I. Abrahams, Scattering of sound by an elastic plate with flow, *Journal of Sound and Vibration* 89 (2) (1983) 213–231.
[7] N. Atalla, J. Nicolas, A formulation for mean flow effects on sound radiation from rectangular baffled plates with arbitrary boundary conditions, *Journal of Vibration and Acoustics* 117 (1995) 22–29.
[8] W. Graham, The effect of mean flow on the radiation efficiency of rectangular plates, *Proceedings of the Royal Society of London* 454 (1998) 111–137.
[9] K. Frampton, Radiation efficiency of convected fluid loaded plates, *Journal of the Acoustical Society of America* 113 (5) (2003) 2663–2673.
[10] K. Frampton, The effect of flow induced coupling on sound radiation from convected fluid loaded plates, *Journal of the Acoustical Society of America* 117 (3) (2005) 1129–1137.
[11] F. Sgard, N. Atalla, J. Nicolas, Coupled FEM-BEM approach for mean flow effects on vibroacoustic behavior of planar structures, *AIAA Journal* 32 (12) (1994) 2351–2358.
[12] S. Wu, L. Maestrello, Responses of finite baffled plate to turbulent flow excitations, *AIAA Journal* 33 (1) (1995) 13–19.
[13] A. Frendi, L. Maestrello, A. Bayliss, Coupling between plate vibration and acoustic radiation, *Journal of Sound and Vibration* 177 (2) (1994) 207–226.
[14] E.H. Phillips, Revised Design: Aerion aims for improvements in aerodynamics and cabin comfort, *Aviation Week and Space Technology* 163 (18) (2005) 70.
[15] C. Fenno, A. Bayliss, L. Maestrello, Interaction of sound from supersonic jets with nearby structures, ICASE Report 97-31, June 1997.
[16] L. Meirovitch, *Analytical Methods in Vibrations*, Macmillan, New York, 1967.
[17] A. Leissa, *Vibration of Plates*, Acoustical Society of America, American Institute of Physics, New York, 1993.
[18] R. Clark, W. Saunders, G. Gibbs, *Structures: Dynamics and Controls*, Wiley, New York, 1998.
[19] C. Wallace, Radiation resistance of a rectangular panel, *Journal of the Acoustical Society of America* 51 (3 (Part 2)) (1972) 946–952.
[20] M. Currey, K. Cunefare, The radiation modes of baffled finite plates, *Journal of the Acoustical Society of America* 98 (3) (1995) 1570–1580.
[21] S. Kung, A New Identification and Model Reduction Algorithm via Singular Value Decomposition, *IEEE 12th Asilomar Conference on Circuits, System and Computers*, Pacific Grove, CA, November 1978, pp. 705–714.
[22] A. Pierce, *Acoustics, An Introduction to it's Physical Principles and Applications*, Acoustical Society of America, American Institute of Physics, New York, 1991.
[23] N. Peake, Nonlinear stability of a fluid loaded elastic plate with mean flow, *Journal of Fluid Mechanics* 434 (2001) 101–118.
[24] L. Maestrello, T. Linden, Response of an acoustically loaded panel excited by supersonically convected turbulence, *Journal of Sound and Vibration* 16 (3) (1971) 365–384.
[25] A. Frendi, L. Maestrello, On the combined effect of mean flow and acoustic excitation on structural response and radiation, *Journal of Vibrations and Acoustics* 119 (1997) 448–456.
[26] F. Bauer, L. Maestrello, L. Ting, Acoustic field in unsteady moving media, *Journal of the Acoustical Society of America* 99 (3) (1996) 1291–1305.